MECHANICAL ANALOG OF QUBITS

Fabius Tan Choon Keong[1], Xie Yundi[2], Wee Wei Hsiung[3]
[1]River Valley High School, 6 Boon Lay Ave, Singapore 649961
[2]Raffles Institution, 1 Raffles Institution Lane, Singapore 575954
[3]DSO National Laboratories, 2 Science Park Dr, Singapore 118225

1. Abstract

Quantum mechanics is a field of physics notorious for it being difficult to visualise, especially when considering quantum information in the form of classical physics. The objective of this project is to design a mechanical analog of a Qubit that allows us to demonstrate the ability to manipulate its orientation through an applied magnetic field, in order to better visualise how a Qubit works. In this paper, a magnetised gyroscope is freely suspended, then spun up using a motor. When this gyroscope is placed in a uniform magnetic field generated by surrounding coils, the precession of the gyroscope can be controlled and monitored. Through several trials, it was observed that the precession of the gyroscope could be controlled by varying the strength of the magnetic fields, and that the stronger the magnetic field, the greater the effect on the precession of the gyroscope. By simulating the behaviour of a Bloch sphere under the influences of external magnetic fields, the magnetised gyroscope can be used as a classical representation of a quantum phenomenon. Due to the set-up's little need of mathematical formulae, the magnetised gyroscope may prove especially useful for understanding fundamental concepts of quantum mechanics at an introductory level.

2. Introduction

Qubits, or quantum bits, are the basic units of quantum information found in the form of a two-state quantum-mechanical system. They are essential in the advancement of our current computing power, with initial quantum coprocessor algorithms such as Shor's Algorithm potentially being able to surpass the mathematical prowess of current classical computers [1].

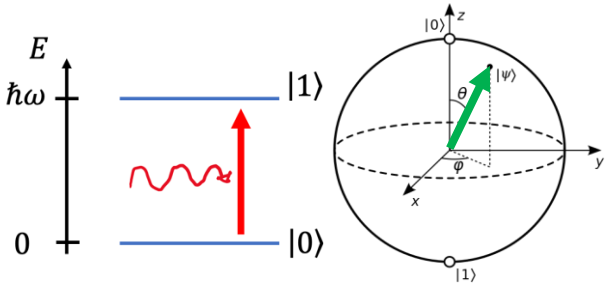

Figure 1: Energy levels of a Qubit (Left) and a Bloch representation of the Qubit state (Right)

To define a qubit, we note that it is a two-state system. The Qubit can be represented as seen in Figure 1. However, what differentiates the Qubit from a regular Bit lies in the curved line drawn in the above figure – an external electromagnetic field (EMF). For a regular bit, there exists 2 similar states, 0 and 1. However, the states of a Qubit are not constrained to these 2 states. Rather, when an EMF is applied onto the Qubit, the states can be manipulated, allowing the quantum states to superpose and be described by a linear combination of both states, i.e. $|\psi\rangle = \alpha|0\rangle + \beta|1\rangle$ [2].

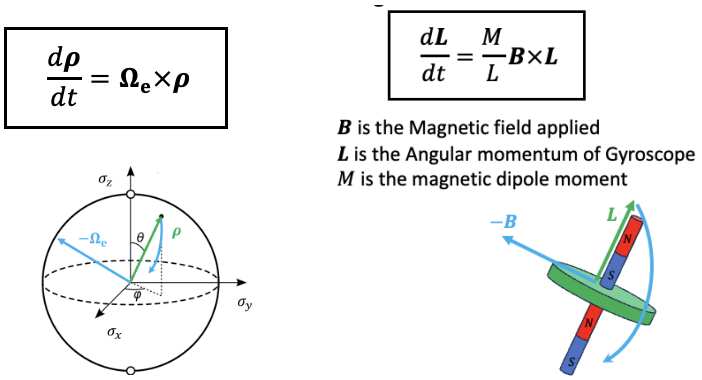

Figure 2: Equivalence of Qubits (Left) and Magnetic Gyroscopes (Right)

Instead, a more conventional method involves mapping the motion of a gyroscope onto Qubit dynamics, due to their innate similarities, as can be observed in Figure 2. Utilising a magnetised gyroscope with external magnetic fields applied onto it, it is possible to demonstrate that its subsequent motion can be observed and mapped directly onto Qubit dynamics. Through this seemingly simple model, various applications of the Qubit can be demonstrated from the mere ability of preparing, manipulating and reading these Qubits — for instance, Nuclear Magnetic Resonance Imaging (NMRI). Specifically, by mapping a gyroscope, we can potentially provide a clearer demonstration of how current real-life qubits are applied, like in NMRIs.

This "motion" is defined as precession, and to understand it, we utilise this simplified depiction of a magnetised gyroscope (Annex A). Note that magnets are attached in the diagram, making it a magnetic gyroscope, which is similar to our set-up, in which we attached permanent magnets to the gyroscope holder. As we spin the gyroscope, we create a change in angular momentum, $\frac{d\boldsymbol{L}}{dt}$,

where **L** is the angular momentum of the gyroscope. We can derive an equation $\frac{d\boldsymbol{L}}{dt} = \frac{M}{\boldsymbol{L}}\boldsymbol{B} \times \boldsymbol{L}$,

where M is the magnetic dipole moment of the gyroscope and **B** is the magnetic field applied by the coils that we place beside the gyroscope. The torque produced by the external magnetic field is known to be perpendicular to the vector **L**, as it attempts to reorientate the direction of the vector, given by $d\boldsymbol{L} = \tau\, dt$. However, the gyroscope will attempt to resist this change in position, resulting in precession about the vertical axis about the gyroscope.

3. Materials and Methods

3.1 Objectives and variables considered

The objective of this project was to design a mechanical analog of a Qubit that allows us to demonstrate the ability to manipulate its orientation through an applied magnetic field and is mainly done through utilising a magnetised gyroscope. Figure 3.1 lists all the variables that we considered for our set-up.

As we are investigating the orientation of the Qubit due to the magnetic fields, the minimum distance between the magnets and the gyroscope is an essential consideration for a magnetic gyroscope. To obtain this distance, we measured the strength of the magnets used (3100 Gauss) to determine the extent of its generated magnetic field, before placing the gyroscope just out of the range of the magnetic field generated. This is done as the magnetic field was found to be a significant factor affecting the rate of precession of a gyroscope in its range but is not a factor that we intend to investigate [6]. As such, the minimum distance would be 76.1cm. However, we note that if the gyroscope is made of a non-magnetic material, such a factor need not be considered, as the magnets will not affect the precession in any way, apart from the change in weight of the whole system.

For any type of coils used, a minimum current had to be determined and administered to allow for multiple sets of data whilst accounting for the maximum current that can run through them. More importantly, this consideration will help ensure that we can achieve an initial torque on the gyroscope, to induce a change in the angular momentum of the gyroscope [8]. Hence, we tested and concluded that the minimum voltage administered should be 1.000A.

Variable	**Symbol**	**Value**
Distance between magnets and gyroscope	D_{MG}	76.1 cm
Minimum current administered to the coils	A_C	1.000 A

Figure 3.1: Table of variables considered for our set-up

3.2 Selection of coils for set-up

For the generation of our magnetic fields, Helmholtz coils were initially selected over conventional choices such as electromagnets, which provide flexibility through easy adjustments of the magnetic field strength but have a lack of uniformity for the magnetic field generated, which restricts the measurements that can be taken and therefore the accuracy of our experiment.

However, preliminary trials showed that they may not be successful for the range of currents that we intend to use (1.000A – 2.000A). This was confirmed through placing permanent magnets on a non-magnetic plastic plate, then situated in the centre of the coils used. We set the current to the same range that we intend to investigate for the actual experiment and found that the permanent magnets barely reorientated themselves even when displaced by angles of up to 90°. This implied that the magnetic field generated by the Helmholtz coils used may have been too weak. Hence, we created a second set-up using solenoids to surround our magnets, which could provide stronger magnetic fields (Annex B).

3.3 Structural features of Gyroscope set-up

For our holder for the gyroscope and any other 3D printed parts, we first designed it on Fusion360 (Annex C) before 3D printing it out of PLA+ filament (Polylactic acid). PLA+ was favoured over other options such as acrylonitrile butadiene styrene (ABS) plastic, mainly due to its tensile strength. PLA+ has a tensile strength of 57.8MPa (Filament World), while ABS has a tensile strength of 28.3MPa (Curbell Plastics). Having a higher tensile strength, it will help ensure that the gyroscope is not accidentally angled below the vertical axis when weight is applied, which may cause the rotor to unintentionally "precess" more than it should be under the magnetic field applied.

For our gyroscope, we considered 3 choices (Annex D):

A. Solid brass with a lightweight aluminium frame (148.4g)
B. Solid brass with a triaxial brass frame (557.7g)
C. Fully printed out of PLA+ filament (25.8g)

Choice A was ultimately chosen in favour of B and C due to the ease of rotation and number of axes. As the conventional method of measuring the ease of rotation of a gyroscope requires specialised equipment that we did not have access to, we sought an alternative. To determine the extent of "ease", we utilised our phone cameras to capture trial rotations in slow-motion. We made sure to apply a similar amount of force when rotating the rotor of each gyroscope, before analysing the number of rotations in 5 seconds, where the gyroscope with most ease was the one with the most rotations. A was found to have the most "ease".

In terms of the number of axes, this was an essential consideration, as it would determine the direction of rotation [10]. A was biaxial (2 orthogonal axes), while both B and C were triaxial (3 orthogonal axes). For our research, B and C would have been better options for ease of observing the precession due to their smaller error margins as triaxial gyroscopes [16], but due to high levels of friction noted between the axes and B's high weight, we worked with the biaxial A.

3.4 Balance of moments

As the weight of the attached magnets do not fully cancel out the weight of the whole holder, there is a net clockwise moment on the whole system. A counterweight was then added with the magnets to generate a counter-moment, stabilising our set-up, and ensuring that the precession we observe was not due to this net moment on the system. Upon calculations, we attached a counterweight of mass 1.40g (Annex E).

3.5 Attaching the components

To ensure that the axes of our gyroscope can freely rotate, we designed a set-up to suspend the gyroscope by means of strings attached to the outer frame of the gyroscope (Annex F). We then measured and marked the direct centre between the relevant solenoids/coils, allowing us to maintain a consistent position of our gyroscope, which is essential in ensuring that the gyroscope does not deviate in position across all datasets taken.

4. Results

After the parts were all fully assembled, the coils were then powered by a Multicomp Pro power supply, which applied an initial current of 1.000A. A camera was then set up to capture the motion of the gyroscope at 120 frames per second (FPS). A tracker was then used to analyse the angle and rate of precession in the gyroscope through the frames of the videos. We conducted 4 trials, as listed below.

4.1 Analysis of first trial

Our first trial involves the Helmholtz coil method, which in theory worked. However, when trialled, we found that the magnetic field generated by the Helmholtz coils was far too weak to allow us to note any observable precession in our gyroscope

4.2 Analysis of second trial

Therefore, we dismantled the Helmholtz coil set up and instead tried to push the spinning gyroscope. In Figure 4.2, the left diagram is labelled with the magnetic field applied by the permanent magnets, B, the 2 magnets M_1 and M_2 , the axis of rotation, the angular momentum vector L, as well as the direction of precession. As seen in the figure, upon spinning up the gyroscope, the magnets were observed to have a significant effect on precession of the gyroscope.

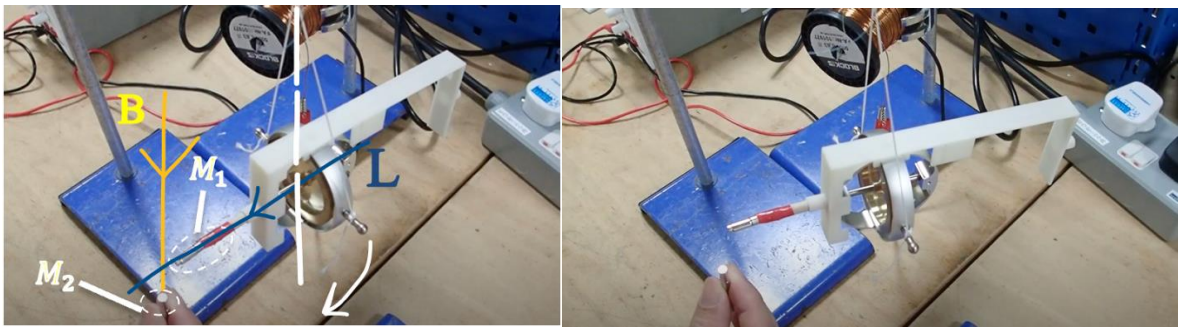

Figure 4.2: Comparison of effect by permanent magnet on gyroscopic precession (Left refers to earlier time, Right refers to observation after 1.0s)

4.3 Analysis of third trial

We then moved onto using homemade solenoids using copper coils (Annex H). From Figure 4.3, we observe the magnetic field, B, exiting the page and the same variables as in Figure 4.2, and we found that the higher the magnetic field strength, the greater the precession. When the positive and negative terminals were switched, reversing the current flow, the gyroscope was also observed to precess in the opposite direction. This proved that the precession of the gyroscope could be controlled in precise ways by changing the direction and magnitude of the magnetic field.

Figure 4.3: Homemade solenoids used to control gyroscopic precession (Left refers to earlier time, Right refers to observation after 1.0s)

4.4 Analysis of fourth trial (rate of precession)

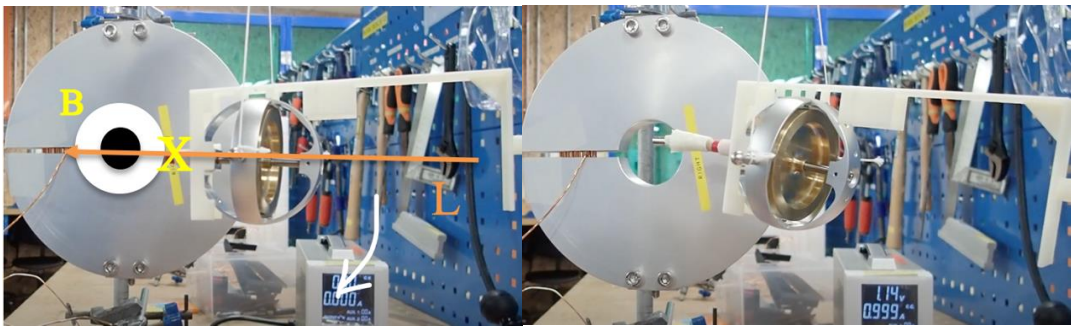

Figure 4.4: Coiled solenoids used to control gyroscopic precession (Left refers to earlier time, Right refers to observation after 1.0s)

Upon swapping out the Helmholtz coils for coiled solenoids (Annex I), we observe a trend relating the magnetic field strength to the rate of precession. Figure 4.4 shows the gyroscope undergoing precession, as depicted by the curved white arrow.

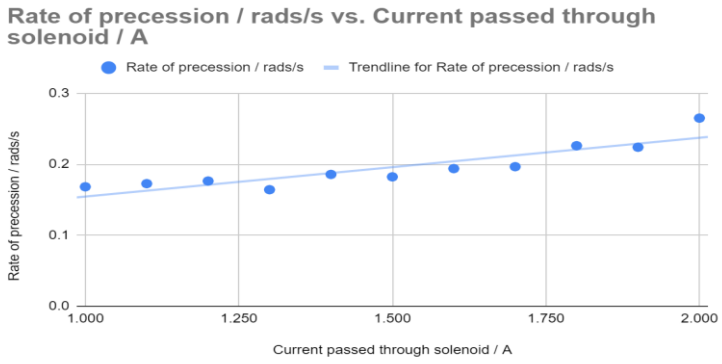

Figure 4.5: Comparison of rate measured at varying currents

From Figure 4.5, there is an evidently approximate proportional correlation between the rate of precession and the magnetic field strength of the magnetic field induced by the solenoid, since

the current applied is directly proportional to the strength of the magnetic field (Magnetic field formula), thus corroborating with our hypothesis.

However, some points may appear as anomalies that do not fit the general trend. This is due to rocking motions of the gyroscope set-up when the gyroscope was wound up, which could not be prevented due to the nylon strings used. These caused uncertainties in the reference points taken when starting the tracker, resulting in variations in starting and ending points of the gyroscope's tracked motion.

4.5 Analysis of fourth trial (Angle of precession)

We used Davinci Resolve's tracking feature to analyse the video taken of the precession of the gyroscope with the solenoid set at 1.500A. Through the tracking feature, we managed to observe the motion of the gyroscope and observe that it was approximately 35°. Unfortunately, due to limitations in capturing videos, we were not able to measure the angles of precession at varying currents through the solenoids.

5. Discussion

5.1 Observing precession

From the analysis, we found that the magnetic field induced externally onto the gyroscopes indeed had a roughly proportional effect on the rate of precession of the gyroscope, aligning with our theory and hypothesis. As seen from our analysis, the gyroscope underwent precession as expected when a torque was applied.

Referring back to Section 3.1, as our gyroscope used was made of brass and aluminium, which are both non-magnetic, when testing the gyroscope with magnets, the magnets were not attracted to any part of the gyroscope, thus the magnets placed beside the gyroscope did not affect the precession that we observed in our trials, ensuring the reliability of our results.

However, empirical data to support further currents induced could not be obtained past 2.000A as our gyroscope could not undergo precession along a uniform path without losing control. Hence, the stability of our set-up has to be improved by adjusting the position of the strings attached to a more ergonomic position that does not restrict further precession, or by changing the type of string used to one that better fits our agenda. These will help us conduct further testing on the gyroscope.

5.2 Mapping results onto qubit dynamics

To tie our results to the idea of Qubits, as in our main objective, we utilise the idea of Bloch Spheres, which are geometrical representations of the pure state space of a Qubit. Bloch Spheres allow us to represent the Qubit, a 2-level quantum system, through its three-dimensions. The state Qubit can be represented by a Density Matrix $\hat{\rho}$, where $\hat{\rho} = |\psi\rangle\langle\psi|$. $\hat{\rho}$ can be further re-expressed as $\frac{1}{2}(\mathbf{1} + \boldsymbol{\rho} \cdot \boldsymbol{\sigma})$. $\boldsymbol{\sigma} = [\sigma_x, \sigma_y, \sigma_z]$, the Pauli matrices, which account for the spin of the object in an applied magnetic field, while $\boldsymbol{\rho}$ is simply a 3-Dimensional vector representing a state on the Bloch Sphere. We conclude that $\frac{d\rho}{dt} = \Omega_e \times \rho$ (Annex J), where Ω_e is the Rabi frequency, the rate at

which the Qubit oscillates between the 2 orthogonal states, $|0\rangle$ and $|1\rangle$. With these equations, we calculate the rotation rate of the Qubit through our analog and effectively bridge the gap between Qubit and mechanical dynamics.

6. Limitations and future work

Due to the constraints such as a lack of access to specialised equipment, the system could not be calibrated to the precision desired, limiting the accuracy of the data we obtained. Future work could explore the possibility of accelerometers or replacing the material of the strings holding up the gyroscope and its holder with one that less restricts the precession, in order to accurately measure the angular displacement of our gyroscope and tune its precision. Time constraints also prevented us from investigating other in-depth variables, so future studies could explore the effects of Mu metal shields to shield the gyroscope from the magnetic fields, along with exploring the effects of reducing friction between the spin axes on the change in angular momentum observed.

7. Acknowledgement

Finally, we would like to acknowledge those in DSO that have been with us and have guided us throughout the project, namely, Desmond, staff of DSO and our mentor Dr Wee Wei Hsiung for imparting their knowledge and skills onto us**.**

8. References

[1]Classiq (2022). *Quantum Cryptography - Shor's Algorithm explained.*

https://www.classiq.io/insights/shors-algorithm-explained

[2]Wikipedia (n.d.) *Qubit.* Retrieved 31 December 2023 from https://en.wikipedia.org/wiki/Qubit

Aritro Pathak (2016). *An elementary argument for the magnetic field outside a solenoid.* Retrieved November 29, 2023, from

https://iopscience.iop.org/article/10.1088/0143-0807/38/1/015201/pdf

Michael A. Nielsen, Isaac L. Chuang (2010). *Quantum Computation and Quantum Information*

https://books.google.com.sg/books?hl=en&lr=&id=-s4DEy7o-a0C&oi=fnd&pg=PR17&dq=A+Short+Introduction+to+Quantum+Information+and+Quantum+Computation&ots=NJ1FdmsB_s&sig=tVyjvsqKn53WmEH296mShCy8NYU&redir_esc=y#v=onepage&q&f=false

Michel Le Bellac (2006). *A short introduction to quantum information and*

quantum computation

https://dokumen.tips/documents/a-short-introduction-to-quantum-information-and-qu

antum-computation-michel-le-bellac.html?page=1

Turner, G. (n.d.). *Gyroscopes - Everything you needed to know*. Copyright 2015 (All Web Pages) by Glenn Turner. http://www.gyroscopes.org/how.asp

John S. Townsend (2012). *Modern Approach To Quantum Mechanics by John S. Townsend*

https://www.softouch.on.ca/kb/data/Modern%20Approach%20to%20Quantum%20Mechanics%202E%20(A).pdf

[7]Department of Physics and Astronomy, University of Alabama (2009). *Problem Set 5*

https://pleclair.ua.edu/ph126/Homework/F09/HW5_2oct09_SOLN.pdf

[8]MIT 8.01 *3-Dimensional Rotation: Gyroscopes*

https://web.mit.edu/8.01t/www/materials/Presentations/old_files_f07/Presentation_W13D2.pdf

M.C. Mott-Smith. (n.d.). *The friction of the Gyroscope: How to eliminate it.*

https://adsabs.harvard.edu/pdf/1922PA.....30..390M

[10] Marshall Brain (2023). *How the Gyroscope works.* Retrieved 6 December 2023 from

https://science.howstuffworks.com/gyroscope.htm

Mark Looney (n.d). *A simple calibration for MEMS Gyroscopes*

https://www.analog.com/media/en/technical-documentation/technical-articles/GyroCalibration_EDN_EU_7_2010.pdf

Li Wang et al. (2021). *An efficient calibration method for Triaxial Gyroscopes.*

https://arxiv.org/pdf/2103.11096.pdf

UCLA Physics & Astronomy (n.d.). *Rotation and Gyroscopic Precession.* Retrieved 6 December 2023 from

https://demoweb.physics.ucla.edu/sites/default/files/Physics6A_Exp7_0.pdf

Jian Sun et al. (2022). *Mechanics of the Gyroscopic Precession and Calculation of the Galactic Mass.* Retrieved 6 December 2023 from

https://www.scirp.org/journal/paperinformation.aspx?paperid=114730

Pavel Fadeev et al. (2021). Quantum Sci. Technol. *Ferromagnetic gyroscopes for tests of fundamental physics.* Retrieved 6 December 2023 from

https://iopscience.iop.org/article/10.1088/2058-9565/abd892/ampdf

[16]Foreign Technology Division, USSR (1982). *Gyro Systems*

https://apps.dtic.mil/sti/tr/pdf/ADA113748.pdf

Wikipedia (n.d.) *Precession.* Retrieved 31 December 2023 from https://en.wikipedia.org/wiki/Precession

Wikipedia (n.d.) *Density Matrix.* Retrieved 31 December 2023 from https://en.wikipedia.org/wiki/Density_matrix

Wikipedia (n.d.) *Pauli matrices.* Retrieved 31 December 2023 from https://en.wikipedia.org/wiki/Pauli_matrices#Physics

Wikipedia (n.d.) *Pauli matrices.* Retrieved 31 December 2023 from https://en.wikipedia.org/wiki/Interaction_picture

9. Annex

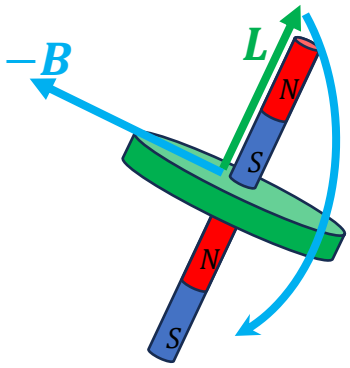

Annex A: Depiction of magnetised gyroscope

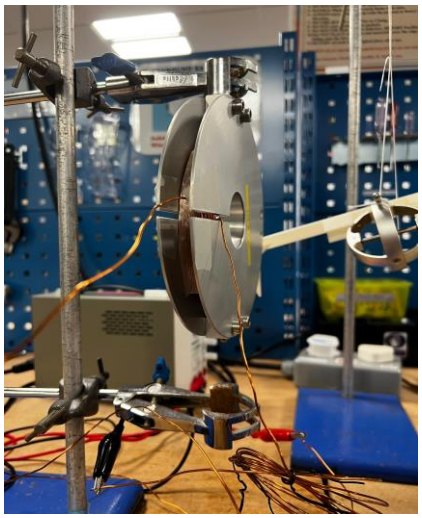

Annex B: Coiled solenoids

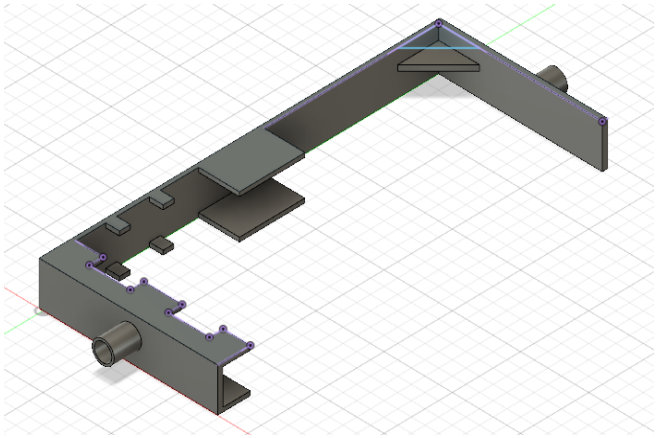

Annex C: 3D model of the custom gyroscope stand

A B

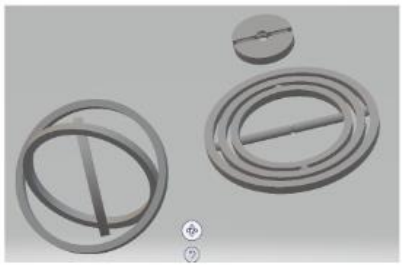

C

Annex D: Pictures of the 3 models of gyroscopes considered

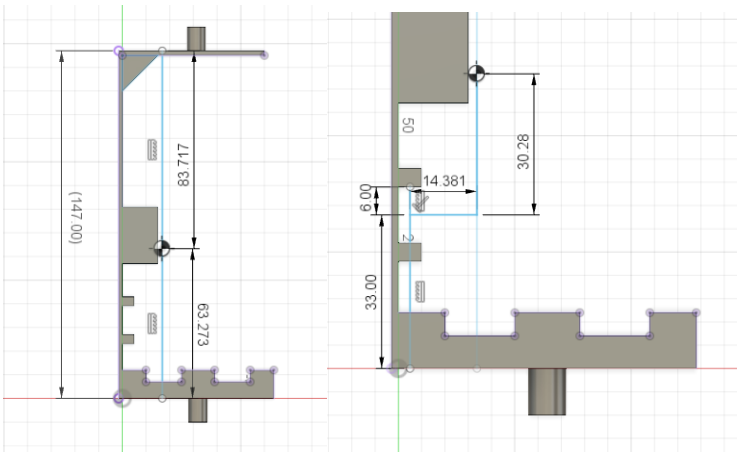

Using Fusion360, we can find the centre of gravity of the holder, allowing us to precisely measure the mass of counterweight needed, $Mass_{CW}$, which was found to be 1.40 g.

Annex E: Calculation of mass of counterweight required to achieve static equilibrium

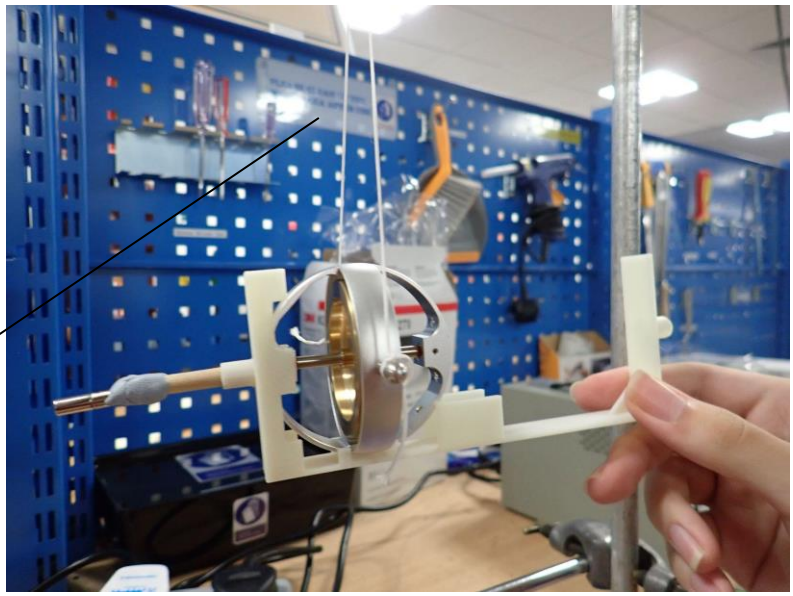

Annex F: Strings attached to the gyroscope

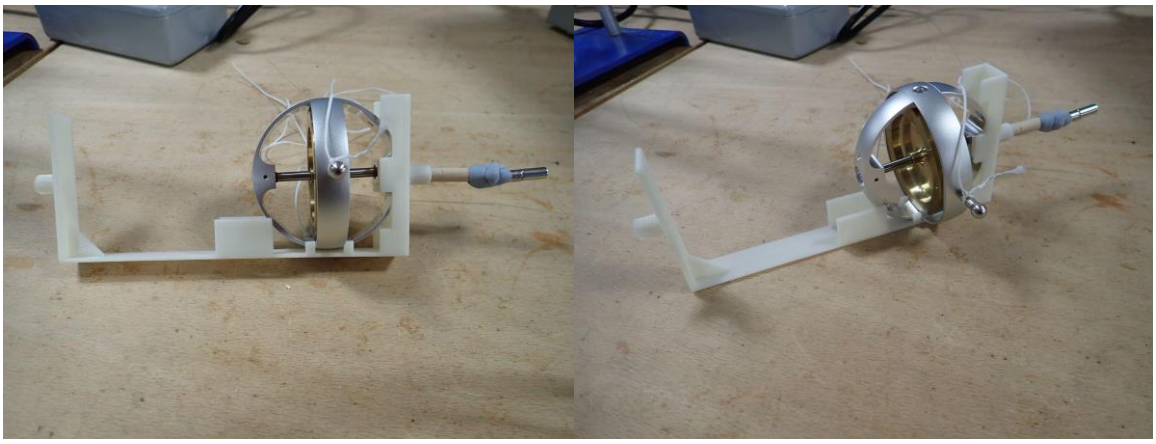

Annex G: Custom holder for gyroscope

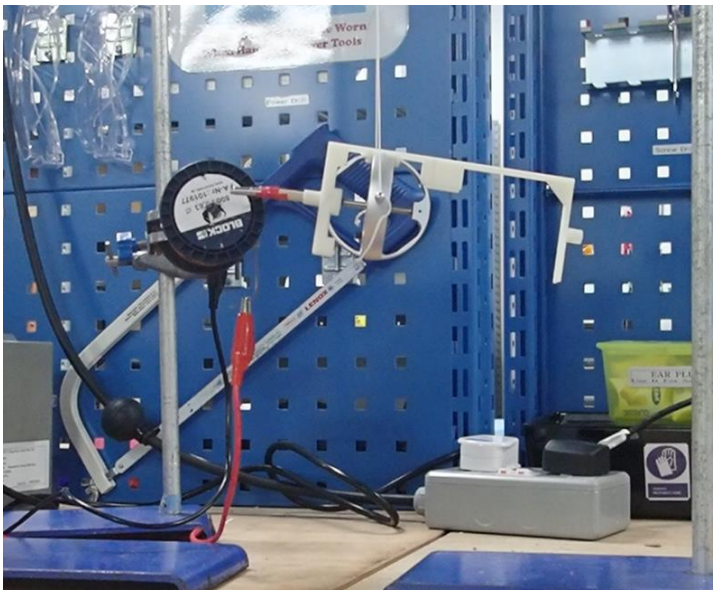

Annex H: Full set-up of homemade solenoid method

Annex I: Full set-up of Solenoid method

The Pauli Matrices obey the commutation relationship $[\sigma_i, \sigma_j] = 2i\sigma_k$.

Quantum Mechanics tells us that the Density matrix evolves in a manner where

$$\frac{d\hat{\rho}}{dt} = \frac{1}{i\hbar}[\hat{H}, \hat{\rho}]$$

$$\hat{H} = \boldsymbol{H} \cdot \boldsymbol{\sigma}$$

$\hat{H}$ is the Hamiltonian, a representation of the total energy of the system.

By the Pauli Matrices,

$$[\hat{H}, \hat{\rho}] = i(\boldsymbol{H} \times \boldsymbol{\rho}) \cdot \boldsymbol{\sigma}$$

$$\frac{d\hat{\rho}}{dt} = \frac{1}{i\hbar}[\hat{H}, \hat{\rho}]$$

$$= \boldsymbol{\Omega_e} \times \boldsymbol{\rho}$$

Where $\boldsymbol{H} = \hbar\boldsymbol{\Omega_e}$ represents the rotation rate of the gyroscope.

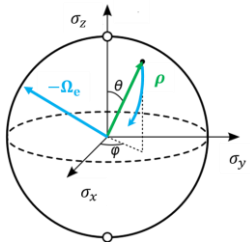

The diagram above shows the interactions of all the above variables, where $\boldsymbol{\Omega_e} = \Omega\sigma_x + \Delta\sigma_z$, in which Ω is the Rabi frequency and Δ is the detuning from the resonance frequency.

Annex J: Derivation of $\frac{d\boldsymbol{\rho}}{dt} = \boldsymbol{\Omega_e} \times \boldsymbol{\rho}$

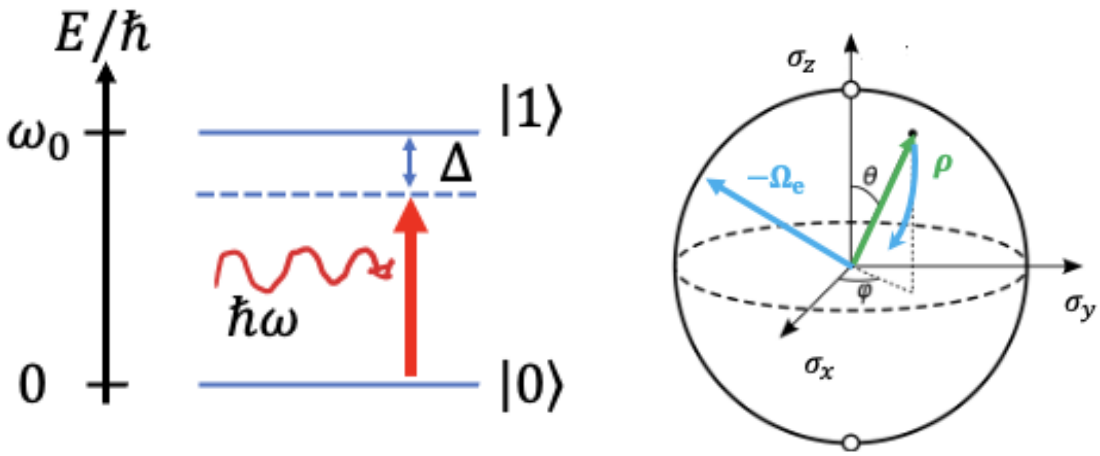

Annex K: Energy level of a Qubit and a Bloch representation of a Qubit state

2.1 Introduction to gyroscopic precession

Gyroscopes are devices mounted on a frame and able to sense an angular velocity if the frame is rotating. Many classes of gyroscopes exist, depending on the operating physical principle and the technology involved. Precession is the change of angular velocity and angular momentum produced by torque. In most cases when gravitational forces are involved, the angular momentum of the object decreases, causing the axle to spin in smaller and smaller circles

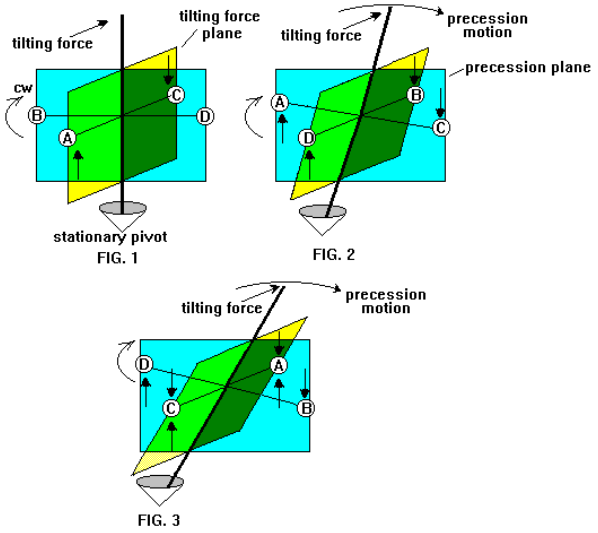

Figure 2: A gyroscope with 2 degrees of freedom

To be more specific, a gyroscope with 2 degrees of freedom can be moved left, right, front and back, and through this, rotate and precess. From Figure 2 and in FIG. 1, 4-point masses, A, B, C, D, represent the areas along the rim of the gyroscope. When a tilting force is applied to the top axis, A is sent in an upward direction and C goes in a downward direction, as seen in FIG. 2. Since this gyroscope is rotating in a clockwise direction, point A will be where point B was when the gyroscope has rotated 90 degrees. The same goes for point C and D. Point A is still traveling in the upward direction when it is at the 90 degrees position in FIG. 2 and point C will be traveling in the downward direction. The combined motion of A and C cause the axis to rotate in the "precession plane" to the right (FIG 2). Note that a gyroscope's axis will move at a right angle to a rotating motion.

When the gyroscope has rotated another 90 degrees, point C is now where point A was at when the tilting force was first applied, as seen in FIG. 3. The downward motion of point C is now countered by the tilting force and the axis does not rotate in the "tilting force" plane. The more the tilting force pushes the axis, the more the rim on the other side pushes the axis back when the rim revolves around 180 degrees. When points A and C finally make it around to the opposite sides, the tilting force is more than the upward and downward counter acting forces.

Annex L: Understanding precession